Proceedings of the ASME 2013 International Design Engineering Technical Conferences & Computers and Information in Engineering Conference
IDETC/CIE 2013
August 4-7, 2013, Portland, Oregon, USA

DETC2013-13196

SENSITIVITY OF ARRAY-LIKE AND OPTIMIZED WIND FARM OUTPUT TO KEY FACTORS AND CHOICE OF WAKE MODELS

Weiyang Tong[*]
Syracuse University
Syracuse, NY 13244
Email: wtong@syr.edu

Souma Chowdhury[†]
Syracuse University
Syracuse, NY 13244
Email: sochowdh@syr.edu

Ali Mehmani[*]
Syracuse University
Syracuse, NY 13244
Email: amehmani@syr.edu

Jie Zhang[‡]
Syracuse University
Syracuse, NY 13244
Email: jzhang56@syr.edu

Achille Messac[§]
Syracuse University
Syracuse, NY 13244
Email: messac@syr.edu

ABSTRACT

The creation of wakes, with unique turbulence characteristics, downstream of turbines significantly increases the complexity of the boundary layer flow within a wind farm. In conventional wind farm design, analytical wake models are generally used to compute the wake-induced power losses, with different wake models yielding significantly different estimates. In this context, the wake behavior, and subsequently the farm power generation, can be expressed as functions of a series of key factors. A quantitative understanding of the relative impact of each of these factors is paramount to the development of more reliable power generation models; such an understanding is however missing in the current state of the art in wind farm design. In this paper, we quantitatively explore how the farm power generation, estimated using four different analytical wake models, is influenced by the following key factors: (i) incoming wind speed, (ii) land configuration, and (iii) ambient turbulence. The sensitivity of the maximum farm output potential to the input factors, when using different wake models, is also analyzed. The extended Fourier Amplitude Sensitivity Test (eFAST) method is used to perform the sensitivity analysis. The power generation model and the optimization strategy is adopted from the Unrestricted Wind Farm Layout Optimization (UWFLO) framework. In the case of an array-like turbine arrangement, both the first-order and the total-order sensitivity analysis indices of the power output with respect to the incoming wind speed were found to reach a value of 99%, *irrespective of the choice of wake models. However, in the case of maximum power output, significant variation (around 30%) in the indices was observed across different wake models, especially when the incoming wind speed is close to the rated speed of the turbines.*

KEYWORDS: Fourier Amplitude Sensitivity Test, Mixed-discrete Particle Swarm Optimization, power generation, Unrestricted Wind Farm Layout Optimization, wake model

[*]Doctoral Student, Multidisciplinary Design and Optimization Laboratory, Department of Mechanical and Aerospace Engineering. ASME Student Member

[†]Research Assistant Professor, Multidisciplinary Design and Optimization Laboratory, Department of Mechanical and Aerospace Engineering. ASME Member.

[‡]Currently at the National Renewable Energy Laboratory (NREL), Golden, CO 80401. ASME Member.

[§]Distinguished Professor and Department Chair, Department of Mechanical and Aerospace Engineering, ASME Lifetime Fellow. Corresponding Author.

INTRODUCTION

Wind energy is one of the fastest growing renewable energy. The energy from wind is generally harvested through wind farms, which can consist of hundreds of turbines. In practice, the power generated from a wind farm is always less than that by the sum of all installed turbines when operating as standalone entities. This power reduction is mainly attributed to the wake effect, which causes velocity deficits downstream of a turbine. In the case of wind farm design, wake models have been widely used to evaluate this wake-induced power reduction. The effectiveness of the power estimation of the concerned wind farm therefore relies on the accuracy and the reliability of the wake model used. To this end, an understanding of turbine wakes is crucial to the estimation of wind farm power generation.

Wind Farm Power Estimation

As the wind flows across a turbine, the available power generated can be given by

$$P_0 = C_P \frac{1}{2} \rho A U^3 \tag{1}$$

where P_0 represents the available power generation; C_P is the power coefficient; ρ is the air density; A is the rotor swept area expressed as $\frac{\pi D^2}{4}$, where D is the rotor diameter; and U is the wind velocity immediately in front of the turbine. The IEC 61400-12-1 provides a standard approach to measure the power curve of a single turbine [1]. It is observed that the rotor diameter and the velocity immediately in front of the turbine are influential to the single turbine power output: the power available in a stream of wind flowing across a turbine is proportional to the area swept by the turbine rotor, as well as the cube of the velocity immediately in front of the turbine.

The case becomes extremely challenging when we estimate the power generation of a wind farm, in which the power generation of a wind farm depends on the power performance not only of each single turbine but of the complete wind farm. Various factors can influence the wind farm power output, such as turbine availability, electrical efficiency, curtailments, etc. [2]. Among those energy loss factors, the influence from the wake effect is undoubtedly significant. The creation of turbine wakes not only causes velocity deficits on downstream turbines, it also increases the complexity of the Atmospheric Boundary Layer (ABL) flow within a wind farm. Hence, the wind farm power generation is indirectly caused by the factors that regulate the behavior of turbine wakes. Generally, these factors can be classified into two categories: the natural factors and the design factors.

The natural factors are primarily the variation in wind conditions (including wind speed, wind shear, and ambient turbulence) at the concerned farm site (as reflected by the nature of wind), which are **uncontrollable**. In a real wind farm, the wind conditions can vary from one location to another; especially for a complex terrain case, the wind conditions can change drastically over a short distance (e.g., 1 *km*) [3]. The design factors, such as turbine locations, turbine characteristics (*e.g.*, rotor diameter, hub height), and land configuration (*e.g.*, land area, land shape), are generally **controllable** or planned for the purpose of avoiding energy losses (particularly referred to the wake-induced energy loss) in the design of wind farms. These general knowledge, however, leads to several important specific questions, such as:

1. What is the relative impact of these factors?
2. Does the impact of these factors on the wind farm power output vary when using different wake models?
3. Is it the controllable factors or the uncontrollable factors that drive most of the variation of the wind farm power output?

An extensive Sensitivity Analysis (SA) of the wind farm power output to these two types of factors is performed in this paper, in seeking to address the above questions. A clear understanding of how sensitive the farm output to each input factor is also essential to improve the accuracy of wind farm power estimation. In this paper, we use four different analytical wake models, including the Jensen model, the Frandsen model, the Larsen model, and the Ishihara model, to examine how the impact of these factors vary with the choice of wake models.

Sensitivity Analysis in Wind Farm Design

Sensitivity analysis (SA) is the study of how the variation in the output of a model can be apportioned, qualitatively or quantitatively, to different sources of variation, and of how the given model depends upon the information fed into it [4,5]. For a given model, SA can help determine which of the input factors result in the most significant impact on the output of this model.

Some work has been done in the general area of sensitivity analysis with different aspects of wind farm dynamics to important factors. Rocklin and Constantinescu [6] presented an approach to estimate the adjoint sensitivity of wind power generation using numerical weather prediction (NWP) models. Osborn et al. [7] analyzed the sensitivity of wind development, in National Energy Modeling System (NEMS) to a series of assumptions that affect wind resource development. Rose and Hiskens [8] used trajectory sensitivities to quantify the effects of individual parameters on the dynamic behavior of wind turbine generators. Zack et al. [9] performed the ensemble sensitivity analysis of the wind speed forecast regarding changes in the prior values of atmospheric state variables. Capps et al. [10] evaluated the sensitivity of the energy production of a wind farm (southern California) to the variations in key turbine characteristics, including hub height, rated power, rotor diameter, and turbine characteristic incremental costs.

In this paper, we analyze the sensitivity of the wind farm output to the following key factors at the farm site level: (i) in-

coming wind speed, (ii) land configuration, (iii) nameplate capacity, and (iv) the ambient turbulence. Given that the addressed problem has a low number of input factors and requires a relatively high computational cost per system evaluation, a variance-based method, the extended Fourier Amplitude Sensitivity Test (eFAST), is used in this paper to perform the SA.

MODELS AND METHODS

Power Generation Model

The power generation model used in this paper is adopted from the Unrestricted Wind Farm Layout Optimization (UWFLO) framework [11]. This power generation model quantifies the wind farm power output as a function of turbine characteristics, turbine locations, and incoming wind conditions. The power output of each turbine is evaluated based on its order of encountering incoming wind flow. An influence matrix is created to determine if a turbine is affected by the wake effect. For a $N-$turbine wind farm, Turbine-j is in the influence of the wake created by Turbine-i if and only if

$$\begin{gathered}\Delta x_{ij} < 0 \text{ and } \sqrt{(\Delta y_{ij})^2 + (\Delta H_{ij})^2} - \frac{D_j}{2} < \frac{D_{wake,ij}}{2}, \\ \Delta x_{ij} = x_i - x_j,\ \Delta y_{ij} = y_i - y_j,\ \Delta H_{ij} = H_i - H_j \\ \forall i, j = 1, 2, \ldots, N, i \neq j\end{gathered} \tag{2}$$

where the single index i or j indicates the corresponding turbine number; x and y represent the turbine coordinates; H represents the hub height of the corresponding turbine; and $D_{wake,ij}$ is the wake width (created by Turbine-i) at the location of Turbine-j.

A *generalized power curve* is used to evaluate the power output of each turbine. This *generalized power curve* is scaled back to represent the approximated power response of a particular commercial turbine, using its specifications. In this case, the power generated from a single turbine (P) can be evaluated using the following equations [12]:

$$\frac{P}{P_r} = \begin{cases} P_n\left(\frac{U-U_{in}}{U_r-U_{in}}\right), & if\ U_{in} < U < U_r \\ 1, & if\ U_r < U < U_{out} \\ 0, & if\ U_{out} < U\ or\ U < U_{in} \end{cases} \tag{3}$$

where P_r is the turbine rated capacity; U_{in}, U_{out}, and U_r are turbine's cut-in, cut-out, and rated speeds, respectively; and P_n represents the polynomial fit for the *generalized power curve*.

Another feature of this model is that it uses a variable induction factor. According to the 1-D flow assumption, the induction factor a and the power coefficient C_P can be related by

$$C_P = 4a(1-a)^2 \tag{4}$$

where the power coefficient can be expressed as a function of incoming wind speed and turbine characteristics, as given by

$$C_P = \frac{P}{P_0} = \frac{P}{\frac{1}{2}\rho\pi\frac{D^2}{4}U^3} \tag{5}$$

Subsequent solution of the non-linear equation (Eq. 4) gives the induction factor for each turbine with estimated approaching wind conditions.

The Katic model [13] is used here to account for the wake merging. Partial wake overlapping is also uniquely accounted for. If Turbine-j is in the influence of multiple wakes created by K upstream turbines, the corresponding velocity deficit v_j is given by

$$v_j = \sqrt{\sum_{k=1}^{K} \frac{A_{kj}}{A_j}\left(U_j - U_{kj}\right)^2} \tag{6}$$

where U_{kj} represents the wake speed (created by Turbine-k) at the location of Turbine-j; and A_{kj} is the effective influence area of wake (created by Turbine-k) on Turbine-j. If Turbine-j is completely in the wake of Turbine-k, $A_{kj} = A_j$; otherwise, A_{kj} denotes the overlapping area between the wake of Turbine-k and Turbine-j. Thereafter, the overall power output of a N-turbine wind farm, P_{farm}, can be calculated as

$$P_{farm} = \sum_{j=1}^{N} P_i \tag{7}$$

The farm capacity factor, CF, is used in this paper to quantify the power performance. The farm capacity factor is defined as the ratio of the actual power generation to the nameplate capacity of the farm site, which can be expressed as

$$CF = \frac{P_{farm}}{P_{NC}} \tag{8}$$

where P_{NC} is the nameplate capacity of the concerned wind farm.

Wake Models

Two types of wake models are commonly used in simulating flows inside a wind farm: (i) analytical and (ii) computational wake models. In the analytical wake model (as shown in Fig. 1), a set of analytical expressions are used to mathematically describe the behavior of turbine wakes. Although computational wake models use complete Computational Fluid Dynamics

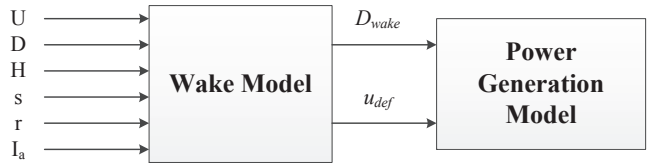

FIGURE 1. General inputs and outputs of an analytical wake model

(CFD) analysis (dictated by the Navier-Stokes equations) to characterize the flow more accurately, their use is limited to the study of single turbine cases. In the context of wind farm layout optimization, the wake models need to simulate the wake behavior of all installed turbines for thousands of candidate farm layouts. Compared to computational wake models, analytical models are thus preferred for their computational efficiency in wind farm layout optimization problems.

In this paper, we implement four analytical wake models to quantify the wake-induced power reduction, which are: Jensen model, Larsen model, Frandsen model, and Ishihara model. Table 1 lists the general input factors considered in each wake model. The description of each wake model will be presented in the following subsections.

Jensen Model The analytical wake model developed by Jensen and later reported by Katic [13, 14] is one of the oldest analytical wake models. The key assumptions in this model are that the wake behind the wind turbine has a linear expansion, and the velocity deficit is only dependent on the distance downstream from the turbine. The wake growth is formulated as

$$D_{wake} = D(1+2ks) \tag{9}$$

where s is the normalized downstream distance (with respect to the rotor diameter) behind the turbine. The velocity deficit v in the (fully developed) wake is expressed as

$$v = U\left[\frac{1-\sqrt{1-C_T}}{(1+2ks)^2}\right] \tag{10}$$

where C_T is the thrust coefficient; and the parameter k is the wake decay constant, which represents how the wake breaks down by specifying the growth of the wake width per unit length in the downstream direction.

Larsen Model The Larsen wake model was first recommended in the European Wind Turbine Standards II (EWTS II) 1999 report for use in wake load calculations [15, 16]. In this model, the Prandtl's mixing length theory is applied, and the wake flow is assumed to be incompressible, stationary and axisymmetric. The velocity deficit, depending on both the radial distance (r) and the downstream distance from the turbine (x), can be formulated as

$$v = -\tfrac{U}{9}\left[C_T A(x+x_0)^{-2}\right]^{\frac{1}{3}}\left\{r^{\frac{3}{2}}\left[3c_1^2 C_T A(x+x_0)\right]^{-\frac{1}{2}} - \left(\tfrac{35}{2\pi}\right)^{\frac{3}{10}}(3c_1^2)^{-\frac{1}{5}}\right\}^2 \tag{11}$$

where A is the rotor swept area.

The wake growth in the Larsen model is given by

$$D_{wake} = 2\left(\frac{35}{2\pi}\right)^{\frac{1}{5}}(3c_1^2)^{\frac{1}{5}}\left[C_T A(x+x_0)\right]^{\frac{1}{3}} \tag{12}$$

where c_1 is a constant that represents the non-dimensional mixing length (related to the Prandtl's mixing length); and x_0 is another constant that denotes the turbine's position with respect to the applied coordinate system. The formulae used to estimate these two constants are given by [17]

$$c_1 = \left(\frac{D_{eff}}{2}\right)^{\frac{5}{2}}\left(\frac{105}{2\pi}\right)^{-\frac{1}{2}}(C_T A x_0)^{-\frac{5}{6}} \tag{13}$$

$$x_0 = \frac{9.5D}{\left(\frac{2R_{9.5}}{D_{eff}}\right)^3 - 1} \tag{14}$$

where D_{eff} is the effective rotor diameter given by

$$D_{eff} = D\sqrt{\frac{1+\sqrt{1-C_T}}{2\sqrt{1-C_T}}} \tag{15}$$

and $R_{9.5}$ represents the wake radius at a relative distance of 9.5 rotor diameters ($9.5D$) downstream from the turbine, which is defined as

$$R_{9.5} = 0.5\left[R_{nb} + min(H, R_{nb})\right] \tag{16}$$

where R_{nb} is an empirical expression related to the ambient turbulence (I_a),

$$R_{nb} = max(1.08D, 1.08D + 21.7D(I_a - 0.05)) \tag{17}$$

TABLE 1. Inputs to each wake model

Input of wake model	Jensen	Frandsen	Larsen	Ishihara
Incoming wind speed	✓	✓	✓	✓
Downstream distance from the turbine	✓	✓	✓	✓
Radial distance from the turbine			✓	✓
Rotor diameter	✓	✓	✓	✓
Hub height			✓	
Turbulence intensity			✓	✓

Frandsen Model The Frandsen model adopted in the Storpark Analytical Model (SAM) is originally used to predict the wind speed deficit in large offshore wind farms with a rectangular site area and equal spacing of the wind turbines [18]. In this model, the turbine wake is assumed to have three impacting regimes. The wake growth in the first regime is given by

$$D_{wake} = D\left(\beta^{k/2} + \alpha s\right)^{1/k} \tag{18}$$

with the wake expansion parameter β formulated as

$$\beta = \frac{1+\sqrt{1-C_T}}{2\sqrt{1-C_T}} = \left(\frac{D_{eff}}{D}\right)^2, \quad s = x/D \tag{19}$$

where the parameter α describes the initial wake expansion, and the value of k is 2 (square root shape) [18, 19]. For the velocity deficit, it is formulated as

$$v = \frac{U}{2}\left(1 \pm \sqrt{1 - 2\frac{A}{A_{wake}}C_T}\right) \tag{20}$$

where A_{wake} is the effective influence area of the wake with respect to the wake width at the current location. In the "$\pm$" sign, the "+" applies to cases in which the induction factor $a \leq 0.5$, while the "$-$" applies to $a > 0.5$.

Ishihara Model The Ishihara model is developed using wind tunnel data for a scaled model of a Mitsubishi wind turbine [20] . The velocity profile of Ishihara model is assumed to have a Gaussian profile, and the velocity deficit is given by

$$v = \frac{\sqrt{C_T}U}{32}\left(\frac{1.666}{k_1}\right)^2 \left(\frac{x}{D}\right)^{-p} \exp\left(-\frac{r^2}{{D_{wake}}^2}\right) \tag{21}$$

where the wake growth is formulated as

$$D_{wake} = \frac{k_1 C_T^{\frac{1}{4}}}{0.833} D^{1-\frac{p}{2}} x^{\frac{p}{2}} \tag{22}$$

The parameter p is a function of two forms of turbulence, as given by

$$p = k_2(I_a + I_w) \tag{23}$$

where I_a and I_w represent the ambient turbulence and the turbine-induced turbulence, respectively. The turbine-induced turbulence can be expressed as

$$I_w = \frac{k_3 C_T}{max(I_a, 0.03)}\left\{1 - \exp\left[-4\left(\frac{x}{10D}\right)^2\right]\right\} \tag{24}$$

Here, the coefficients k_1, k_2, and k_3 are respectively set to 0.27, 6.0, and 0.004 as found in the literature [20, 21].

The Extended Fourier Amplitude Sensitivity Test

The Extended Fourier Amplitude Sensitivity Test (eFAST) developed by Saltelli and Bolado [22] is a variance-based SA method. This method is based on the original FAST method [23–26]. In the original FAST method, the input factors of a model are transformed into a frequency domain by Fourier transformation. Thus, a multi-dimensional model is reduced into a single dimension. For a model with m input factors, $X_1, X_2, \ldots, X_m$, the output of the model, Y, can be expressed as

$$Y = f(X_1, X_2, \ldots, X_m) \tag{25}$$

By assigning a frequency ω_j, each input factor can be transformed into a frequency domain spanned by a scalar s, as follows

$$X_i = G_i(sin\omega_i s); \qquad i = 1, 2, \ldots, m, \tag{26}$$

Therefore, the model output can be represented by its expectation, $E(Y)$, which can be approximated as

$$E(Y) = \frac{1}{2\pi}\int_{-\pi}^{\pi} f(s)ds \tag{27}$$

where $f(s) = f(x_1(s), x_2(s), \ldots, x_m(s))$. By using the properties of Fourier series [23], an approximation of the variance of the output, s_Y^2, can be given by

$$\begin{aligned} s_Y^2 &= \frac{1}{2\pi}\int_{-\pi}^{\pi} f^2(s)ds - [E(Y)]^2 \\ &\approx 2\sum_{j=1}^{\infty}(A_j^2 + B_j^2) \end{aligned} \tag{28}$$

where

$$A_j = \frac{1}{2\pi}\int_{-\pi}^{\pi} f(s)\cos jsds \tag{29}$$

$$B_j = \frac{1}{2\pi}\int_{-\pi}^{\pi} f(s)\sin jsds \tag{30}$$

The first-order indices provide a way to rank individual input factors on the basis of their contribution to the variance of the output. They are computed by evaluating the A_j and B_j for the fundamental frequency ω_i and its higher harmonics denoted by $p\omega_i$ for $p = 1, 2, \ldots, \infty$. Hence, the conditional variance s_{Y/X_i}^2 can be approximated by

$$s_{Y/X_i}^2 \approx 2\sum_{p=1}^{\infty}(A_{p\omega_i}^2 + B_{p\omega_i}^2) \tag{31}$$

Since the Fourier amplitudes decrease as the value of p increases; s_{Y/X_i}^2 can thus be further approximated by

$$s_{Y/X_i}^2 = 2\sum_{p=1}^{M}(A_{p\omega_i}^2 + B_{p\omega_i}^2) \tag{32}$$

where M is the maximum harmonic, and is normally taken to be 4 or 6 [25]. Therefore, the first-order indices denoted by S_i are calculated as the ratio of the conditional variance of each input factor to the variance of the output (s_i^2), as given by

$$S_i = \frac{s_{Y/X_i}^2}{s_i^2} \tag{33}$$

The primary advantage of the eFAST method over the original FAST is its ability to deal with the total-order indices of the input factors, which includes the interactions between the input factors of any order. The basic idea behind the computation of the total-order indices by the eFAST method is to consider the frequencies that do not belong to the set $\{p_1\omega_1, p_1\omega_2, \ldots, p_m\omega_m\}$ for $p_i = 1, 2, \ldots, \infty$ and $\forall i = 1, 2, \ldots, m$. Here, we use $\neq i$ to represent all except i [4]. By doing so, the conditional variance, $s_{Y/X_{\neq i}}^2$, can be expressed as

$$s_{Y/X_{\neq i}}^2 = 2\sum_{p=1}^{M}(A_{p\omega_{\neq i}}^2 + B_{p\omega_{\neq i}}^2) \tag{34}$$

Therefore, the total-order indices are given by

$$S_{Ti} = 1 - \frac{s_{Y/X_{\neq i}}^2}{s_i^2} \tag{35}$$

Mixed-Discrete Particle Swarm Optimization

The sensitivity of the maximum potential farm output to the key input factors is also analyzed in this paper. To maximize the farm output, we use the Mixed-Discrete Particle Swarm Optimization (MDPSO) algorithm developed by Chowdhury et al. [27]. One prominent advantage that the MDPSO algorithm has over a conventional PSO algorithm is that it has the diversity preservation capability to prevent premature stagnation of particles. The basic steps of the advanced algorithm are summarized as

$$x_i^{t+1} = x_i^t + v + i^{t+1} \tag{36}$$

$$\begin{aligned} v_i^{t+1} = {} & \alpha v_i^t + \beta_l r_1(p_i - x_i^t) + \beta_g r_2(p_g - x_i^t) \\ & + \gamma r_3(x_i^t - p_g) \end{aligned} \tag{37}$$

where x_i^t and v_i^t represent the position and the velocity of the i^{th} particle at the t^{th} generation, respectively; r_1, r_2, and r_3 are random numbers between 0 and 1; p_i is the best candidate solution found for the i^{th} particle; p_g is the best candidate solution for the entire population (swarm); α, β_l, and β_g are user defined constants that are respectively associated with inertial weight, exploitation, and exploration; γ is the diversity preservation coefficient that is evaluated adaptively as a function of the prevailing diversity in the population at the concerned iteration. This diversity preservation coefficient is scaled using an user defined parameter, γ_0. The last term in Eq. 37 decelerates the motion of particles towards p_g, i.e., the global best, thereby maintaining diversity and preventing premature convergence.

Such an explicit diversity preservation operator is often necessary for solving complex optimization problems that involve

multimodal criterion functions and a large number of design variables, as is the case with the maximization of the farm output presented in this paper. Further discussion of the estimation of the population diversity and the formulation of the diversity coefficient γ can be found in Ref. [27, 28].

TABLE 2. GE 1.5xle Turbine [29]

Specifications	Value
Rated capacity	1500 kW
Cut-in	3.5 m/s
Cut-out	20 m/s
Rated speed	11.5 m/s
Rotor diameter	82.50 m
Swept Area	5346 m^2
Hub height	80 m

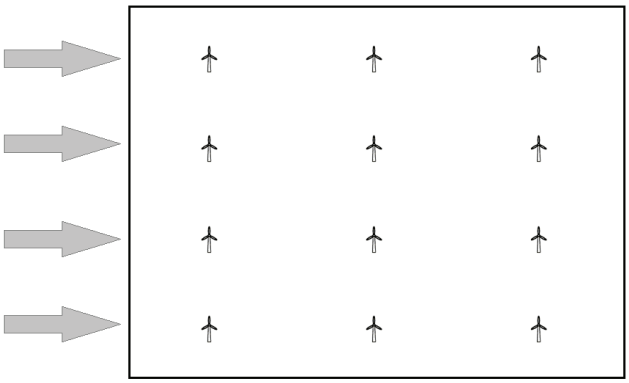

FIGURE 2. An array-like farm layout with 12 GE 1.5-82.5 turbines

SENSITIVITY ANALYSIS OF WIND FARM OUTPUT

In this paper, the sensitivity of wind farm output (the estimated farm power generation and the farm capacity factor) to a series of input factors of the wind farm power generation model is analyzed. Specifically, these input factors include (i) incoming wind speed, (ii) ambient turbulence, (iii) Land Area per MW Installed (LAMI), (iv) Land Aspect Ratio (LAR), and (v) nameplate capacity. It is noted that these factors can also affect the wake effect. Two numerical experiments are conducted to perform the sensitivity analysis, and GE 1.5-82.5 turbines are used. The turbine specifications are listed in Table 2.

A few assumptions are made for both the numerical experiments:

- the wind farm has a rectangular shape.
- the incoming wind is unidirectional (from left to right as shown in Fig. 2).
- identical turbines are installed.
- the incoming wind speed is uniformly distributed over the entire rotor area.
- the ambient turbulence over the farm site is constant everywhere.

In the following subsections, we perform the sensitivity analysis (i) of the estimated power generation for a grid-like turbine array and (ii) of the optimized wind farm output, i.e., the maximum farm capacity factor.

Numerical Experiment I: Wind Farm Power Estimation of an array-like Farm Layout

This experiment analyzed the sensitivity of the estimated farm power output to four input factors, including (i) incoming wind speed (U), (ii) ambient turbulence (I_a), (iii) LAMI (A_{MW}), and (iv) LAR (a_r). A set of 1000 sample input points are generated within the specified ranges as shown in Table 3. The incoming wind speed is ranged from the turbine cut-in speed (3.5 m/s) to the turbine cut-out speed (20 m/s). The LAMI is specified using the following formula [30]

$$10\frac{D^2}{P_r} < A_{MW} < 30\frac{D^2}{P_r}, \quad for\ P_{NC} \in (10P_r, 50P_r) \tag{38}$$

where P_{NC} represents the nameplate capacity of the concerned farm site. Since the wind farm has a rectangular shape, it is assumed that its short side has a minimum length of $1.5D$. Based on the range of LAMI specified in Eq. 38, the upper bound and the lower bound of LAR are 20 and 0.075, respectively. Finally, the ambient turbulence is ranged from 1% to 25%. This range is set based on the measured data used in the literature as well as in the IEC 61400-1 standard.

Totally, there are 12 GE 1.5-82.5 turbines installed on the farm site maintaining an array-like layout of 3×4 or 4×3. The wind farm is divided into 12 identical sub-rectangles, and each turbine is located at the center of each sub-rectangle. The area of each sub-rectangle is regulated by the Land Area per Turbine (LAT), A_T which is given by

$$10D^2 < A_T < 30D^2 \tag{39}$$

TABLE 3. List of input factors of the power generation model.

Input		Minimum	Maximum
Incoming wind speed	Region I	$3.5\ m/s$	$10.35\ m/s$
	Region II	$10.35\ m/s$	$12.65\ m/s$
	Region III	$12.65\ m/s$	$20\ m/s$
Ambient turbulence		1%	25%
Land Area per MW Installed		$45,000\ m^2/MW$	$135,000\ m^2/MW$
Land aspect ratio		0.1	20
Nameplate capacity		$15\ MW$	$75\ MW$

Hence, the length (l) and the width (w) of each sub-rectangle can be calculated as

$$l = \sqrt{A_T a_r}$$
$$w = \sqrt{A_T / a_r} \tag{40}$$

Based on the typical nature of a turbine power curve, the incoming wind speed is divided into three regions as given in Table 3. The first region is below the turbine's rated speed, where the power output is highly sensitive to incoming wind speed variations. The second region is a transient region, which ranges from 10% below the turbine's rated speed to 10% above the rated speed. In this transient region, based on the degree of the wake losses the power output may be highly or weakly sensitive to the incoming wind speed variations. In the third region, the power output is weakly/not sensitive to incoming wind speed variations. Therefore, the sensitivity analysis focuses on the first two regions.

Numerical Experiment II: Wind Farm Power Estimation of an Optimal Farm Layout

In the second numerical experiment, a set of 1000 sample input points are generated to analyze the sensitivity of the optimized farm output. In addition to the previous four input factors, the nameplate capacity (P_{NC}) is selected as a new added input factor in this case. Since identical turbines are used, the number of turbines to be installed can be readily determined if the nameplate capacity is given. Based on Eq. 38, the nameplate capacity is varied from $10P_r$ to $50P_r$ (Table 3), which makes the number of turbines vary from from 10 to 50.

Two cases, Region I and Region II, as specified for the incoming wind speed in the first numerical experiment, are optimized in this experiment. For each case, a set of 1000 sample input factors are generated with the specified range as shown in Table 3. For each combination of the sample input factors, the turbine locations are optimized using the MDPSO algorithm in order to reach a maximum farm output (farm capacity factor). The wind farm layout optimization problem is formulated as follow:

TABLE 4. User-defined parameters in MDPSO

Parameter	Region I	Region II
W	0.5	0.5
β_g	1.5	1.5
β_l	1.5	1.5
γ_{c0}	3.0	5.09
γ_{min}	$1e-4$	$1e-5$
λ	0.15	0.1
Population size	$20 \times N$	$20 \times N$
Max. number of function calls	500,000	600,000

$$\max_{\substack{\vec{X}=[X_1,X_2,\ldots,X_N] \\ \vec{Y}=[Y_1,Y_2,\ldots,Y_N]}} f(\vec{X},\vec{Y}) \tag{41}$$

subject to

$$g(\vec{X},\vec{Y}) \leq \varepsilon \tag{42}$$
$$X_{min} \leq X_i \leq X_{max} \tag{43}$$
$$Y_{min} \leq Y_i \leq Y_{max}$$
$$i = 1,2,\ldots,N$$

where N is the number of turbines; $f(\vec{X},\vec{Y})$ is the objective function of the farm output; and ε deontes the constraint tolerance which is set to $1.0e-6$. Since farm power generation depends on the number of turbines, the farm capacity factor is used as the objective.

TABLE 5. Sensitivity measures for the estimated power output of 3×4 layout

Wake model	Input		Region I		Region II	
			first-order	total-order	first-order	total-order
Jensen	Incoming wind speed	U	0.9990	0.9999	0.9869	0.9996
	Ambient turbulence	I_a	0.0000	0.0011	0.0000	0.0106
	Land area per MW installed	A_{MW}	0.0000	0.0005	0.0000	0.0021
	Land aspect ratio	a_r	0.0000	0.0005	0.0000	0.0021
Frandsen	Incoming wind speed	U	0.9990	0.9999	0.9869	0.9996
	Ambient turbulence	I_a	0.0000	0.0012	0.0000	0.106
	Land area per MW installed	A_{MW}	0.0000	0.0005	0.0000	0.0021
	Land aspect ratio	a_r	0.0000	0.0005	0.0000	0.0021
Larsen	Incoming wind speed	U	0.9989	0.9999	0.9853	0.9990
	Ambient turbulence	I_a	0.0001	0.0012	0.0005	0.0114
	Land area per MW installed	A_{MW}	0.0000	0.0005	0.0000	0.0019
	Land aspect ratio	a_r	0.0000	0.0005	0.0001	0.0022
Ishihara	Incoming wind speed	U	0.9973	0.9987	0.9073	0.9538
	Ambient turbulence	I_a	0.0011	0.0027	0.0442	0.0922
	Land area per MW installed	A_{MW}	0.0000	0.0006	0.0002	0.0097
	Land aspect ratio	a_r	0.0001	0.0007	0.0013	0.0129

Eq. 42 represents the constraint that the minimum spacing (from hub to hub) between any pair of turbines should not be less than $2D$, which is defined in $g(\vec{X},\vec{Y})$ as follows:

$$g(\vec{X},\vec{Y}) = \sum \max\left\{(d_{ij}-2D),0\right\},\ \ i,j=1,2,\ldots,N,\ \textit{and}\ i \neq j \tag{44}$$

where

$$d_{ij} = \sqrt{(X_i - X_j)^2 + (Y_i - Y_j)^2}$$

Eq. 43 defines the boundary of the farm site, which is regulated using LAMI, LAR, and N, as given by

$$\begin{aligned} X_{min} &= 0 \\ Y_{min} &= 0 \\ X_{max} &= \sqrt{NP_r A_{MW} a_r} \\ Y_{max} &= \sqrt{NP_r A_{MW}/a_r} \end{aligned} \tag{45}$$

Results and Discussion

The sensitivity measures for the power output of an array-like wind farm In this experiment, we analyze the sensitivity of the estimated power output of an array-like farm with two different layouts, 3×4 and 4×3, respectively. Table 5 lists the sensitivity measures for the case with a 3×4 layout. In Region I (the incoming wind speed ranges from 3.5 m/s to 10.35 m/s), the incoming wind speed has a decisive impact on the wind farm power output. Both the first-order and the total-order indices of the incoming wind speed reach approximately 99%, irrespective of the choice of wake models. For incoming wind speed variation in Region II, there is a reduction in the relative impact of incoming wind speed. Particularly in the results obtained by the Ishihara model, the first-order index of the incoming wind speed reduces to 89%, while the total-order index reduces to 94%. This is mainly attributed to the consideration of turbine-induced turbulence in this model. Nevertheless, wind farm power output remains significantly sensitive to the incoming wind speed in Region II.

For the case with a 4×3 layout, more turbines located downstream might be in the wakes created by upstream turbines. The results of this case are shown in Table 6. It is observed that the

TABLE 6. Sensitivity measures for the estimated power output of 4×3 layout

Wake model	Input		Region I		Region II	
			first-order	total-order	first-order	total-order
Jensen	Incoming wind speed	U	0.9990	0.9999	0.9869	0.9996
	Ambient turbulence	I_a	0.0000	0.0011	0.0000	0.0106
	Land area per MW installed	A_{MW}	0.0000	0.0005	0.0000	0.0021
	Land aspect ratio	a_r	0.0000	0.0005	0.0000	0.0021
Frandsen	Incoming wind speed	U	0.9990	0.9999	0.9869	0.9996
	Ambient turbulence	I_a	0.0000	0.0011	0.0000	0.106
	Land area per MW installed	A_{MW}	0.0000	0.0005	0.0000	0.0021
	Land aspect ratio	a_r	0.0000	0.0005	0.0000	0.0021
Larsen	Incoming wind speed	U	0.9989	0.9999	0.9848	0.9988
	Ambient turbulence	I_a	0.0001	0.0012	0.0006	0.0117
	Land area per MW installed	A_{MW}	0.0000	0.0005	0.0000	0.0019
	Land aspect ratio	a_r	0.0000	0.0005	0.0001	0.0022
Ishihara	Incoming wind speed	U	0.9968	0.9984	0.8918	0.9453
	Ambient turbulence	I_a	0.0014	0.0031	0.0522	0.1977
	Land area per MW installed	A_{MW}	0.000	0.0007	0.0003	0.0109
	Land aspect ratio	a_r	0.0001	0.0007	0.0015	0.0147

sensitivity measures are basically the same as those in the case with 4×3 layout. This indicates that, as long as the farm layout pattern is fixed, the power output is primarily dependent on the natural factor, the incoming wind speed, rather than the design factors, such as LAMI and LAR (the reflective of turbine spacing).

The sensitivity measures in Region III are not considered. This is because the incoming wind speed in Region III is higher than the turbine's rated speed. Even though turbines are in the wakes created by upstream turbines, they can still operate at their rated capacities. Therefore, the power output is likely to show no/very small variance.

The sensitivity measures for the maximum farm output potential In this experiment, we analyze how the input factors affect the maximum farm capacity factor. The sensitivity measures for the maximum farm output are shown in Table 7. In Region I, the incoming wind speed provides the dominant impact on the maximum capacity factor. However, the relative impact of other input factors vary with the choice of wake models. The sensitivity measures obtained by using the Larsen model and the Ishihara model show that the ambient turbulence has a certain influence due to the consideration of ambient turbulence intensity in both of these two wake models. In the Jensen model, the nameplate capacity has a relatively high influence on the farm output, compared to other input factors.

In Region II, since the small range of the incoming wind speed causes limited variation of the individual turbine power output, other input factors influence the optimized farm output. Given that the Frandsen model predicts the highest wake speed among all of these four wake models [31], it yields the highest values of both the first-order and the total-order indices of the incoming wind speed, which are 92% and 97%, respectively. The ambient turbulence also has a strong impact illustrated by the results when using the Larsen model and the Ishihara model. Especially in the case of the Ishihara model, it is observed that both of the first-order and the total-order indices of the ambient turbulence are somewhat similar to those of the incoming wind speed, which are approximately 51% and 68%, respectively.

It is also important to note that, as the wake model accounts for more inputs (specifically refers to the turbulence in this paper), the sum of the total-order indices becomes larger. This im-

TABLE 7. Sensitivity measures for the maximum farm output potential

Wake model	Input		Region I		Region II	
			first-order	total-order	first-order	total-order
Jensen	Incoming wind speed	U	0.9885	0.9931	0.8224	0.9243
	Ambient turbulence	I_a	0.0001	0.0011	0.0013	0.0161
	Land area per MW installed	A_{MW}	0.0038	0.0075	0.0434	0.1251
	Land aspect ratio	a_r	0.0008	0.0034	0.0045	0.0325
	Nameplate capacity	NC	0.2535	0.5571	0.0209	0.0671
Frandsen	Incoming wind speed	U	0.9950	0.9973	0.9207	0.9696
	Ambient turbulence	I_a	0.0000	0.0003	0.0000	0.0669
	Land area per MW installed	A_{MW}	0.0012	0.0032	0.0138	0.457
	Land aspect ratio	a_r	0.0004	0.0020	0.0045	0.0251
	Nameplate capacity	NC	0.0012	0.0032	0.0108	0.0427
Larsen	Incoming wind speed	U	0.9838	0.9892	0.6888	0.8272
	Ambient turbulence	I_a	0.0167	0.0259	0.2573	0.4286
	Land area per MW installed	A_{MW}	0.0012	0.0042	0.0401	0.1168
	Land aspect ratio	a_r	0.0016	0.0046	0.0225	0.0863
	Nameplate capacity	NC	0.0021	0.0058	0.0533	0.1639
Ishihara	Incoming wind speed	U	0.9864	0.9914	0.5234	0.6885
	Ambient turbulence	I_a	0.0170	0.0276	0.5058	0.6792
	Land area per MW installed	A_{MW}	0.0027	0.0048	0.0863	0.2000
	Land aspect ratio	a_r	0.0022	0.123	0.0058	0.1214
	Nameplate capacity	NC	0.0036	0.0082	0.0793	0.2117

plies that the model to predict the maximum farm capacity factor is non-additive, i.e., the quantification of this model output needs to prudently consider the interaction between the input factors. In contrast, for an array-like farm layout, the power generation is additive, as the sum of the first-order indices of the incoming wind speed is nearly the same as that of its total-order indices.

CONCLUSION

In this paper, we explore the sensitivity of the estimated farm output to five key input factors. By applying the eFAST method, both the first-order and the total-order indices of the input factor impact on the wind farm output can be obtained. We found that if the farm layout is given, the incoming wind speed has a decisive impact on the farm output, irrespective of the choice of wake models. Additionally, the farm output is also sensitive to the incoming wind speed if the incoming wind speed is lower than the turbine rated speed. However, if the incoming wind speed varies within the range close to the turbine's rated speed ($\pm$10% of the rated speed), the optimized farm output becomes more sensitive to design factors, such as the land configuration (LAMI and LAR) and the number of turbines installed.

Moreover, the relative impact of these input factors is strongly dependent on the choice of wake models, especially for wind speeds close to the rated speed. As seen from the Region II column of Table 7, the first-order index of the incoming wind speed reached approximately 92% under the Frandsen model, and only 52% under the Ishihara model. Similarly in Region II, the total-order index of the incoming wind speed under the the Frandsen model reached 97%, as opposed to a mere 69% under the Ishihara model.

Overall, the sensitivity analysis of the power output of both the array-like and the optimized wind farm provides valuable information for the development of high fidelity wake models. Based on the sensitivity measures of each input factor, the accuracy and the reliability of the wake model can be improved with respect to those factors. We also found that the total impact of the natural factors, i.e., the incoming wind speed and the ambient turbulence, drive most of the variance in the farm output. This implies that an accurate wind resource assessment is absolutely crucial to wind farm planning. When the averaged wind speed is close to the turbine's rated speed, the design factors (land configuration and nameplate capacity) have a relatively important impact on the performance of a wind energy project.

Acknowledgements

Support from the National Science Foundation Awards CMMI-1100948, and CMMI-0946765 is gratefully acknowledged. Any opinions, findings, and conclusions or recommendations expressed in this paper are those of the authors and do not necessarily reflect the views of the NSF.

REFERENCES

[1] International Electrotechnical Commission, 2005. IEC 61400-12 wind turbines - part 12-1: Power performance measurements of electricity producing wind turbines. http://www.pewind.com/dateiunterlagen/IEC%2061400-12-1_2005.pdf.

[2] EWEA (European Wind Energy Association), 2009. *Wind Energy − The Facts*. Routledge, ch. I, pp. 51–52.

[3] Albers, A., Gerdes, G., and Deutsches Windenergie-Institut gGmbH (DEWI), Wilhelmshaven (Germany), 1999. "Wind farm performance verification". *DEWI-Magazin,* ***8***(14), pp. 24–35.

[4] Saltelli, A., Chan, K., and Scott, E., 2009. *Sensitivity Analysis*. probability and statistics. Wiley.

[5] Saltelli, A., Tarantola, S., Campolongo, F., and Ratto, M., 2004. *Sensitivity Analysis in Practice: A Guide to Assessing Scientific Models*. Wiley.

[6] Rocklin, M., and Constantinescu, E. M., 2009. Sensitivity of southern california wind energy to turbine characteristics. http://www.mcs.anl.gov/uploads/cels/papers/P1704.pdf.

[7] Osborn, J., Wood, F., Richey, C., Sanders, S., Short, W., and Koomey, J., 2001. A sensitivity analysis of the treatment of wind energy in the AEO99 version of NEMS. Tech. rep., Lawrence Livermore National Laboratory and National Renewable Energy Laboratory, Berkeley, CA, USA.

[8] Rose, J., and Hiskens, I., 2008. "Estimating wind turbine parameters and quantifying their effects on dynamic behavior". In Power and Energy Society General Meeting - Conversion and Delivery of Electrical Energy in the 21st Century, IEEE, pp. 1–7.

[9] Zack, J., Natenberg, E., Young, S., Manobianco, J., and Kamath, C., 2010. Application of ensemble sensitivity analysis to observation targeting for short-term wind speed forecasting. Tech. rep., Lawrence Livermore National Laboratory, Livermore, CA, USA.

[10] Capps, S., Hall, A., and Hughes, M., 2011. Sensitivity of southern california wind energy to turbine characteristics. http://www.atmos.ucla.edu/csrl/publications/Hall/ppr_CaH10.pdf.

[11] Chowdhury, S., Zhang, J., Messac, A., and Castillo, L., 2013. "Optimizing the arrangement and the selection of turbines for wind farms subject to varying wind conditions". *Renewable Energy,* ***52***, pp. 273–282.

[12] Chowdhury, S., 2012. "Integrative modeling and novel particle swarm-based optimal design of wind farms". PhD thesis, Rensselaer Polytechnic Institute, Troy, New York.

[13] Katic, I., Høstrup, J., and Jensen, N., 1987. *A Simple Model for Cluster Efficiency*. A. Raguzzi, pp. 407–410.

[14] Jensen, N., 1983. A note on wind generator interaction. Tech. rep., Risø National Laboratory, Roskilde, Denmark.

[15] Larsen, G., Høstrup, J., and Aagaard Madsen, H., 1996. *Wind fields in wakes*. H.S. Stephens & Associates, pp. 764–768.

[16] Larsen, G., 1988. *A simple wake calculation procedure*. Risø National Laboratory.

[17] Pierik, J., Dekker, J., Braam, H., Bulder, B., Winkelaar, D., Larsen, G., Morfiadakis, E., Chaviaropoulos, P., Derrick, A., and Molly, J., 1999. *European wind turbine standards II (EWTS-II)*. James and James Science Publishers, pp. 568–571.

[18] Frandsen, S., Barthelmie, R., Pryor, S., Rathmann, O., Larsen, S., Højstrup, J., and Thøgersen, M., 2006. "Analytical modelling of wind speed deficit in large offshore wind farms". *Wind Energy,* ***9***(1-2), pp. 39–53.

[19] Barthelmie, R. J., Folkerts, L., Larsen, G. C., Rados, K., Pryor, S. C., Frandsen, S. T., Lange, B., and Schepers, G., 2006. "Comparison of wake model simulations withy offshore wind turbine wake profiles measured by sodar". *Atmospheric and Oceanic Technology,* ***23***(7), pp. 888–901.

[20] Ishihara, T., Yamaguchi, A., and Fujino, Y., 2004. Development of a new wake model based on a wind tunnel experiment. Tech. rep., Global Wind.

[21] Mittal, A., Taylor, L. K., Sreenivas, K., and Arabshahi, A., 2011. "Investigation of two analytical wake models using data from wind farms". In ASME 2011 International Mechanical Engineering Congress and Exposition (IMECE2011), Vol. 6: Fluids and Thermal Systems; Advances for Process Industries, Part A and B, ASME.

[22] Saltelli, A., and Bolado, R., 1998. "An alternative way to compute fourier amplitude sensitivity test (fast)". *Compu-*

tational Statistics & Data Analysis, ***26***(4), pp. 445–460.

[23] Cukier, R. I., Fortuin, C. M., Shuler, K. E., Petschek, A. G., and Schaibly, J. H., 1973. "Study of the sensitivity of coupled reaction systems to uncertainties in rate coefficients. i theory". *Journal of Chemical Physics,* ***59***(8), pp. 3873–3878.

[24] Schaibly, J. H., and Shuler, K. E., 1973. "Study of the sensitivity of coupled reaction systems to uncertainties in rate coefficients. part ii, applications". *Journal of Chemical Physics,* ***59***(8), pp. 3879–3888.

[25] Cukier, R. I., Levine, H. B., and Shuler, K. E., 1975. "Study of the sensitivity of coupled reaction systems to uncertainties in rate coefficients. iii. analysis of the approximations". *Journal of Chemical Physics,* ***63***(3).

[26] Cukier, R. I., Levine, H. B., and Shuler, K. E., 1978. "Nonlinear sensitivity analysis of multiparameter model systems". *Journal of Computational Physics,* ***26***(1), pp. 1–42.

[27] Chowdhury, S., Tong, W., Messac, A., and Zhang, J., 2012. "A mixed-discrete particle swarm optimization algorithm with explicit diversity-preservation". *Structural and Multidisciplinary Optimization*. *DOI: 10.1007/s00158-012-0851-z*, December.

[28] Chowdhury, S., Zhang, J., and Messac, A., 2012. "Avoiding premature convergence in a mixed-discrete particle swarm optimization (MDPSO) algorithm". In 53rd AIAA/ASME/ASCE/AHS/ASC Structures, Structral Dynamics and Materials Conference.

[29] GE Energy, 2009. 1.5MW wind turbine. `http://geosci.uchicago.edu/~moyer/GEOS24705/Readings/GEA14954C15-MW-Broch.pdf`.

[30] Chowdhury, S., Zhang, J., Messac, A., and Castillo, L., 2012. "Characterizing the influence of land area and nameplate capacity on the optimal wind farm performance". In ASME 2012 6th International Conference on Energy Sustainability, ASME.

[31] Tong, W., Chowdhury, S., Zhang, J., and Messac, A., 2012. "Impact of different wake models on the estimation of wind farm power generation". In 12th AIAA Aviation Technology, Integration, and Operations (ATIO) Conference and 14th AIAA/ISSMO Multidisciplinary Analysis and Optimization Conference, American Institute of Aeronautics and Astronautics.